THE JOURNAL OF BIOLOGICAL CHEMISTRY VOL. 286, NO. 40, pp. 34743–34751, October 7, 2011

Interferon-induced Antiviral Protein MxA Interacts with the Cellular RNA Helicases UAP56 and URH49*

Received for publication, April 15, 2011, and in revised form, August 17, 2011 Published, JBC Papers in Press, August 22, 2011, DOI 10.1074/jbc.M111.251843

Christian Wisskirchen[‡§], Thomas H. Ludersdorfer[‡§], Dominik A. Müller[‡], Eva Moritz[‡], and Jovan Pavlovic[‡1]

From the [‡]Institute of Medical Virology and [§]Ph.D. Program in Microbiology and Immunology, University of Zurich, 8057 Zürich, Switzerland

Mx proteins are a family of large GTPases that are induced exclusively by interferon-α/β and have a broad antiviral activity against several viruses, including influenza A virus (IAV). Although the antiviral activities of mouse Mx1 and human MxA have been studied extensively, the molecular mechanism of action remains largely unsolved. Because no direct interaction between Mx proteins and IAV proteins or RNA had been demonstrated so far, we addressed the question of whether Mx protein would interact with cellular proteins required for efficient replication of IAV. Immunoprecipitation of MxA revealed its association with two closely related RNA helicases, UAP56 and URH49. UAP56 and its paralog URH49 play an important role in IAV replication and are involved in nuclear export of IAV mRNAs and prevention of dsRNA accumulation in infected cells. *In vitro* binding assays with purified recombinant proteins revealed that MxA formed a direct complex with the RNA helicases. In addition, recombinant mouse Mx1 was also able to bind to UAP56 or URH49. Furthermore, the complex formation between cytoplasmic MxA and UAP56 or URH49 occurred in the perinuclear region, whereas nuclear Mx1 interacted with UAP56 or URH49 in distinct dots in the nucleus. Taken together, our data reveal that Mx proteins exerting antiviral activity can directly bind to the two cellular DE*x*D/H box RNA helicases UAP56 and URH49. Moreover, the observed subcellular localization of the Mx-RNA helicase complexes coincides with the subcellular localization, where human MxA and mouse Mx1 proteins act antivirally. On the basis of these data, we propose that Mx proteins exert their antiviral activity against IAV by interfering with the function of the RNA helicases UAP56 and URH49.

Mx proteins belong to a family of dynamin-like large GTPases. They play a pivotal role in the type I interferon-mediated response against a broad range of viral infections (1). The human MxA protein accumulates in the cytoplasm and has been shown to inhibit several RNA and DNA viruses, including influenza A virus (IAV),[2] vesicular stomatitis virus, Thogoto virus (THOV), and La Crosse virus (1–3). The murine Mx1 protein is a nuclear protein and inhibits the replication of several members of the orthomyxovirus family, including IAV (1).

Mx proteins share a high intrinsic GTPase activity and the ability to form large oligomeric structures (4). Recently, the crystal structure of the stalk region of MxA was solved, and, in combination with similar structural data from dynamin, a model for a four-helical bundle formation of MxA was proposed (5). It is not clear whether Mx proteins exert their antiviral activity in the form of large oligomeric structures or monomers. Mutations preventing the intermolecular Mx-Mx interactions abrogate the antiviral activity (5), whereas a monomeric form of MxA with a mutation abolishing the intramolecular backfolding of the C-terminal end remains active (6–8). Although the antiviral function of MxA has been studied extensively, little is known about the molecular mechanism of the inhibition. MxA inhibits THOV infection via a physical interaction with the THOV nucleocapsids, blocking the nuclear import of these nucleocapsids (9). For La Crosse virus, an interaction between MxA and the La Crosse virus nucleoprotein was also shown (10). However, for IAV, no direct interaction of Mx proteins with any viral protein could be demonstrated. Hence, we hypothesized that Mx proteins may interfere with the function of cellular protein(s) required for replication of IAV. The human MxA and mouse Mx1 proteins have been shown to associate with several cellular proteins of the cytoskeleton or the proteasomal degradation pathway, but none of these proteins appear to play a role in IAV replication (11, 12). We have shown previously that overexpression of the IAV proteins PB2 and NP (both part of the viral ribonucleoprotein (vRNP) complex) partially overcomes the inhibition of the mouse Mx1 protein (13, 14). More recent studies revealed that the Mx-resistant phenotype of certain influenza virus strains segregates with the NP protein (15, 16). Therefore, we tested whether cellular proteins known to be functionally relevant for the replication of IAV or known to associate with viral proteins or vRNPs (17, 18) would also interact with Mx proteins. For this purpose, we expressed the cDNAs of several cellular proteins (kindly provided by Dr. Peter Palese) that were identified to bind to the nucleoprotein of influenza A (18) in cells transfected with human MxA. Preliminary experiments rapidly revealed that only the DE*x*D/H box RNA helicase Bat-1/UAP56 co-immunoprecipitated with the human MxA protein. UAP56 plays an important role in the assembly of the spliceosome and in nuclear export of spliced and unspliced mRNAs out of the nucleus. It was first described as an essential splicing factor required for spliceosome assembly (19–21). Additionally, UAP56 plays a pivotal role in the nuclear export of mRNA into

* This work was supported by a grant from the Swiss National Science Foundation and a Forschungskredit from the University of Zurich.

[1] To whom correspondence should be addressed: Inst. of Medical Virology, University of Zurich, Winterthurerstr. 190, 8057 Zürich, Switzerland. Tel.: 41-44-634-2656; E-mail: pavlovic.jovan@virology.uzh.ch.

[2] The abbreviations used are: IAV, influenza A virus; THOV, Thogoto virus; vRNP, viral ribonucleoprotein; EGFP, enhanced GFP; GTPγS, guanosine 5′-*O*-(thiotriphosphate).

the cytoplasm (22). Recently, a close paralog of UAP56 termed URH49 (UAP56-related helicase, 49 kDa) was identified that has 90% amino acid identity and exhibits similar cellular functions (23, 24).

Several reports have demonstrated that UAP56 and URH49 also play a role in the efficient replication of IAV (18, 25–27). Momose *et al.* (18) have shown that the interaction of NP with UAP56 leads to increased viral RNA synthesis *in vitro*. In addition, UAP56 and URH49 are required for the efficient export of nascent IAV mRNAs (26, 27), and it was proposed recently that UAP56 is involved in the encapsidation of viral cRNA with NP (25). Moreover, we demonstrated recently that UAP56 is required for the prevention of dsRNA formation during IAV infection, thereby preventing the activation of the type I interferon system (27).

In this study, we provide evidence that human MxA and mouse Mx1 interact with the cellular helicases UAP56 and URH49. *In vitro* studies with recombinant proteins reveal that the interaction is direct. Furthermore co-localization experiments clearly indicate that Mx1 and UAP56 or URH49 form a complex as expected in the cell nucleus whereas the interaction between MxA and UAP56 or URH49 occurs in the cytoplasm.

EXPERIMENTAL PROCEDURES

Cells and Transfections—A549, 3T3, and HEK293T (American Type Culture Collection) cells were cultured in DMEM (Invitrogen) supplemented with 10% FCS, 1% penicillin/streptomycin (Invitrogen), and 1% GlutaMAX (Invitrogen). Cells were transfected at 80% confluency with jetPEI transfection reagent (Polyplus Transfection) as recommended by the manufacturer and incubated for 24 h before being analyzed.

Western Blotting and Co-immunoprecipitation—293T cells were grown in 10-cm cell culture dishes (TPP) and transfected at 80% confluency with the indicated amounts of plasmid. 48 h after transfection, cells were lysed in 500 μl of lysis buffer (0.5% Triton X-100, 20 mM Tris (pH 7.5), 100 mM NaCl, 50 mM β-glycerol phosphate, 50 mM sodium fluoride, 1 mM sodium orthovanadate, and protease inhibitor mixture (Roche Applied Science)). Co-immunoprecipitations were performed with 1 μg of mouse anti-FLAG antibody (Sigma) for 4 h at 4 °C. Immunoprecipitations were done at room temperature for 1 h using 50 μl of protein G beads (Dynabeads, Invitrogen). Samples were washed three times with lysis buffer, and beads were taken up in 40 μl of SDS Laemmli buffer and heated for 5 min to 95 °C. Samples were loaded on 10% SDS gels, followed by immunoblot analysis with different antibodies: mouse and rabbit anti-FLAG (1:3000; Sigma), anti-URH49 (1:750; Acris), anti-UAP56 (serum from a mouse immunized with a peptide of human UAP56), and mouse anti-NP monoclonal HB65 (1:3). Primary antibodies were incubated overnight at 4 °C and incubated the next day for 1 h with HRP-conjugated secondary antibodies (1:10,000; GE Healthcare). Membranes were analyzed on a Fuji imager using MultiGauge Version 3.0 software.

Expression Constructs and Protein Purification—URH49 and UAP56 were cloned into pGEX-3X (GE Healthcare) with an N-terminal GST fusion tag (URH49, 5′-GATAAGAATTCCGCAGAACAGGATGTGGAAAACGATC-3′ (forward; EcoRI) and 5′-CTAATGAATTCAATTTACCGGCTCTGCTCGATGTATGTG-3′ (reverse; EcoRI); and UAP56, 5′-CTTATACCCGGGGCAGAGAACGATGTGGACAATG-3′ (forward; SmaI) and 5′-CAATAATCCCGGGATAAACTACCGTGTCTGTTCAATGTA-3′ (reverse; SmaI). Proteins were expressed in *Escherichia coli* BL21 with 0.1 mM isopropyl β-D-thiogalactopyranoside for 4 h at 32 °C. Bacteria were harvested and lysed by six cycles of sonication for 30 s in 50 mM Tris-HCl (pH 8.0), 500 mM NaCl, 0.1% Nonidet P-40, 5 mM $MgCl_2$, 10 mM 2-mercaptoethanol, 10% glycerol, and protease inhibitor mixture. Lysates were cleared at 12,000 $\times$ *g* for 20 min and applied to a glutathione-Sepharose high performance column (GE Healthcare). Bound proteins were washed with 50 mM Tris-HCl (pH 8.0), 100 mM KCl, 0.1% Nonidet P-40, 5 mM $MgCl_2$, 10 mM 2-mercaptoethanol, and 10% glycerol; eluted with Tris elution buffer (20 mM Tris-HCl (pH 8.0), 100 mM KCl, 0.1% Nonidet P-40, 5 mM $MgCl_2$, 5 mM 2-mercaptoethanol, 10 mM reduced glutathione, and 20% glycerol); and dialyzed against Tris elution buffer without glutathione. His-MxA and His-Mx1 have been described previously (28). Proteins were expressed in *E. coli* M15 (pREP4) cells with 10 μM isopropyl β-D-thiogalactopyranoside for 3 h at 28 °C. Bacteria were harvested and lysed with two French press cycles in 50 mM Tris-HCl (pH 8.0), 500 mM NaCl, 0.1% Nonidet P-40, 5 mM $MgCl_2$, 10 mM 2-mercaptoethanol, 30 mM imidazole, 10% glycerol, and protease inhibitor mixture. Lysates were cleared at 20,000 $\times$ *g* for 20 min and applied to a glutathione-Sepharose high performance column. Bound proteins were washed with 50 mM Tris-HCl (pH 8.0), 100 mM KCl, 0.1% Nonidet P-40, 5 mM $MgCl_2$, 10 mM 2-mercaptoethanol, 30 mM imidazole, and 10% glycerol; eluted with Tris elution buffer (20 mM Tris-HCl (pH 8.0), 100 mM KCl, 0.1% Nonidet P-40, 5 mM $MgCl_2$, 5 mM 2-mercaptoethanol, 300 mM imidazole, and 20% glycerol); and dialyzed against Tris elution buffer without imidazole. The affinity-purified proteins were analyzed on a 10% SDS-polyacrylamide gel. 1 μg of recombinant protein was loaded per lane.

AlphaScreen Assay—The AlphaScreen assay (PerkinElmer Life Sciences) was performed in a 384-well OptiPlate with a 25-μl reaction volume. The recombinant proteins were incubated for 2 h at room temperature at a final concentration of 30 nM each in AlphaScreen buffer (PBS (pH 7.2) and 0.1% BSA) together with AlphaLISA anti-GST acceptor beads and AlphaScreen nickel chelate donor beads at a concentration of 20 μg/ml. Interactions were analyzed on a PerkinElmer EnVision device.

Split GFP System—First, the coding sequence of enhanced GFP (EGFP) amino acids 158–238, including the entire multiple cloning site of pEGFP-C1 (Clontech), was amplified by PCR and ligated into the multiple cloning site of the pcDNA3.1(−)*neo* vector (Invitrogen), yielding vector pcDNA3.1-GFP(158–238). To generate vector pcDNA3.1-GFP(1–157), the coding sequence of EGFP amino acids 158–238 in vector pcDNA3.1-GFP(158–238) was replaced with a PCR product encoding EGFP amino acids 1–157. Subsequently, the open reading frames of human MxA, MxB, UAP56, and URH49 were amplified and introduced in-frame at the 3′-end of the multiple cloning site of EGFP. Expression of the split GFP fusion proteins was verified by Western blot analysis

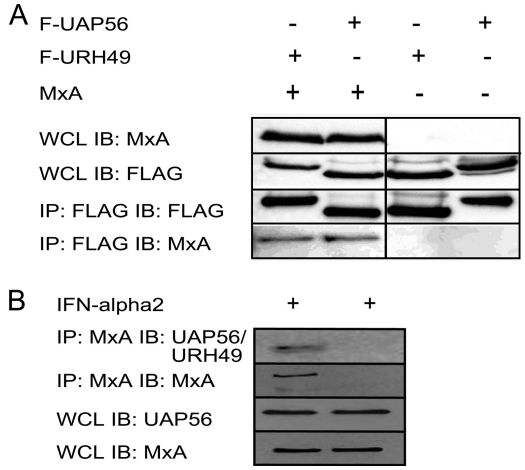

FIGURE 1. **Human MxA interacts with cellular RNA helicases UAP56 and URH49.** *A*, 293T cells were transfected with FLAG-tagged (*F*) UAP56 or URH49 together with MxA, cells were lysed after 48 h, and co-immunoprecipitations were performed using anti-FLAG antibodies. *B*, endogenous co-immunoprecipitations were carried out using A549 cells. For MxA expression, cells were stimulated overnight with 1000 units of interferon-α. Immunoprecipitations (*IP*) were performed from whole cell lysates (*WCL*) using a mouse monoclonal antibody against MxA (*left lane*). A mouse monoclonal antibody against IAV NP was used as a negative control, showing no immunoprecipitation of MxA or UAP56 (*right lane*). *IB*, immunoblot.

using specific antibodies directed against GFP, Mx protein, or UAP56 and URH49.

Indirect Immunofluorescence Analysis—A549 or 3T3 cells were grown on chamber slides for 24 h before being transfected. Cells were fixed with 4% paraformaldehyde and mounted in DAPI-containing mounting medium (Fluoromount-G, SouthernBiotech) when used with the split GFP system. Otherwise, cells were permeabilized with 0.5% Triton X-100 in PBS for 10 min. Cells were washed twice with PBS, and primary and secondary antibodies were diluted in 1% BSA and incubated for 1 h at room temperature. Cells were washed three times after each step. Rabbit anti-FLAG (1:2000) and mouse anti-MxA monoclonal (1:20; clone 143) antibodies were used as primary antibodies. Alexa 488-conjugated anti-rabbit and Alexa 594-conjugated anti-mouse antibodies (1:1000; Invitrogen) were used as secondary antibodies. Slides were mounted in Fluoromount-G mounting medium containing DAPI. Samples were analyzed with a Leica TCS SP5 microscope using LAF software. Quantification of the subcellular distribution of UAP56 or URH49 was performed using ImageJ software.

RESULTS

Co-immunoprecipitation of MxA Protein with UAP56 or URH49—Preliminary experiments aimed at testing several known NP-associated proteins for their capacity to bind to Mx proteins revealed that UAP56, but none of the other cellular proteins tested, interacted with MxA (data not shown). Hence, we first analyzed the interaction of human MxA with UAP56 and its paralog URH49. For this purpose, 293T cells were transfected with plasmids encoding FLAG-tagged UAP56 or URH49 in combination with plasmids encoding MxA. UAP56 and URH49 were immunoprecipitated with anti-FLAG antibody, and the lysates were analyzed by Western blotting (Fig. 1*A*). The data show that both RNA helicases, UAP56 and URH49, interacted with MxA. To eliminate the possibility of a transfection artifact, we also performed co-immunoprecipitations with endogenously expressed proteins. MxA expression was induced in human A549 cells by treatment with interferon-α for 18 h. MxA was immunoprecipitated with anti-MxA monoclonal antibody (isotype IgG2a), and Western blotting with a polyclonal antibody detecting both UAP56 and URH49 was carried out to assess whether UAP56 and/or URH49 was co-precipitated. As a negative control, we carried out an immunoprecipitation using anti-NP monoclonal antibody with the IgG2a isotype as control (Fig. 1*B*). Again, the data clearly indicate that interferon-α-induced MxA formed a complex with UAP56/URH49 (Fig. 1*B*).

Binding of Mx Proteins to UAP56 and URH49 in Vitro—To assess the relative capacity of MxA and Mx1 to bind UAP56 and URH49, we next tested these interactions *in vitro* employing the AlphaScreen assay. For this purpose, recombinant GST-tagged UAP56 or URH49 and His-tagged Mx1 or MxA proteins were expressed in *E. coli* and affinity-purified (Fig. 2*C*). We and others have shown previously that affinity-purified His-tagged Mx proteins exhibit a high intrinsic GTPase activity and antiviral activity *in vitro* (28, 29). For measuring the interaction between Mx proteins and UAP56 or URH49, recombinant proteins (30 nM each in a 25-μl reaction volume) were mixed and incubated together with fluorescently labeled anti-GST acceptor beads and nickel chelate donor beads, resulting in a fluorescence signal upon interaction of only the bead-bound proteins (Fig. 2*A*). Incubation of affinity-purified GST with MxA or Mx1 resulted only in background signal. Quantification of the data revealed a slightly stronger binding of MxA and Mx1 to UAP56 than to URH49 (Fig. 2*A*). Analysis of the affinity-purified proteins on an SDS-polyacrylamide gel revealed that a slightly larger amount of full-length GST-UAP56 than GST-URH49 was present in the protein preparations (Fig. 2*B*), suggesting that the difference in binding was due to the difference in the amount of full-length proteins. The interaction of Mx1 with UAP56 or URH49 yielded a 2–3-fold higher signal than the interaction of MxA with the two helicases (Fig. 2, *A* and *B*). This difference in signal intensity was clearly not due to differences in protein amounts used in the assay (Fig. 2*B*). The additional 30-kDa band seen in the Mx1 protein preparation (Fig. 2*B*) is due to abortive translation at the N terminus of the Mx1 coding sequence (28).

Subcellular Localization of the Complex Formation between Mx Proteins and UAP56 or URH49—MxA exhibits a typical granular staining pattern in the cytoplasm and associates partially with the smooth endoplasmic reticulum (30–32). UAP56 and URH49 accumulate primarily in the nucleus in RNA-splicing speckled domains and nearby nuclear regions, although, for UAP56, there is also evidence for nucleocytoplasmic shuttling (33–35). Hence, we examined in which subcellular compartment the interaction between MxA and UAP56/URH49 takes place. Mouse 3T3 cells were transfected with plasmids encoding MxA and FLAG-tagged URH49 or UAP56. 3T3 cells transfected with MxA protein alone served as negative controls. As expected, UAP56 and URH49 accumulated primarily in the nucleus, forming nuclear speckles, as has been described previously. MxA showed a clear cytoplasmic staining (Fig. 3*A*). Inter-

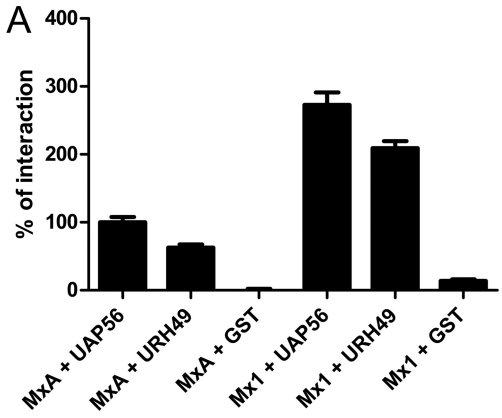

B

	% of interaction
MxA + UAP56	100.00
MxA + URH49	62.95
MxA + GST	0.29
Mx1 + UAP56	272.95
Mx1 + URH49	209.02
Mx1 + GST	13.98

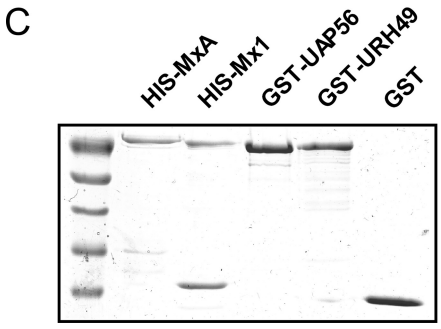

FIGURE 2. ***In vitro* interaction between MxA/Mx1 and UAP56 or URH49.** *A*, affinity-purified GST-UAP56 or GST-URH49 and His-MxA or His-Mx1 (30 nM each protein) were mixed and assayed for interaction *in vitro* using AlphaScreen technology. As a negative control, GST alone was incubated with His-Mx1 or His-MxA. The previously described interaction of UAP56 and MxA was set as a reference for the relative binding strength of the other interactions. *B*, summary of the relative interactions between the proteins in the AlphaScreen assay. *C*, purified proteins were loaded on an SDS gel and Coomassie Blue-stained to show the purity of the protein preparations used in the AlphaScreen assays.

estingly, upon coexpression of MxA with either UAP56 or URH49, we observed accumulation of UAP56 and URH49 also in the cytoplasm of cells expressing MxA (Fig. 3*A*), whereas MxA localization remained unchanged. UAP56 and URH49 were distributed throughout the whole cell. These results indicate that the observed interaction (Figs. 1 and 2) most likely takes place in the cytoplasm.

In addition, we tested whether mouse Mx1 and UAP56 or URH49 would co-localize in the nucleus. Mx1 accumulates in the nucleus in distinct dots, which are in close proximity to polymorphonuclear leukocyte nuclear bodies (36, 37). Immunostaining of cells co-transfected with plasmids coding for Mx1 and FLAG-tagged UAP56 or URH49 indeed revealed a pronounced co-localization of Mx1 with the two RNA helicases (Fig. 3*B*). Moreover, overexpression of Mx1 and the FLAG-tagged RNA helicases did not lead to leakage of these proteins into the cytoplasm (Fig. 3*B*), indicating that the translocation of UAP56 and URH49 into the cytoplasm of MxA-expressing cells is not a transfection artifact.

Nevertheless, we next tested whether endogenous expression of MxA in A549 cells would lead to translocation of a fraction of endogenously expressed UAP56 or URH49 from the nucleus into the cytoplasm (Fig. 4). For this purpose, A549 cells were treated overnight with interferon-α to induce expression of MxA. Immunostaining with antibodies specific for UAP56 (Fig. 4*A*) and URH49 (Fig. 4*B*) revealed that, in the presence of MxA, a small amount of these RNA helicases could indeed be detected in the cytoplasm, whereas the majority of the proteins remained in the nucleus (Fig. 4, *A* and *B*).

To verify that the translocation of UAP56 and URH49 is the result of a complex formation with MxA, we made use of the so-called split GFP system to further study the interaction between MxA and UAP56/URH49. To this end, we adapted a system that has been described previously (38, 39), fusing either the N-terminal region (amino acids 1–157) or the C-terminal region of (amino acids 158–238) EGFP to the N termini of MxA, Mx1, UAP56, and URH49 using a 20-amino acid linker to allow for efficient refolding of the two GFP parts upon interaction of the fusion proteins. UAP56 and URH49 have been described previously to produce homodimers (40), and MxA and Mx1 are able to form homodimers and higher ordered oligomeric structures (reviewed in Ref. 41). Hence, we used the homodimer formation of MxA, Mx1, UAP56, and URH49 proteins fused to the N- and C-terminal regions of GFP as a positive control (Fig. 5, *A* and *B*). As a negative control, we co-transfected plasmids coding for human GFP(1–157)-MxA and human GFP(158–238)-MxB, which are not able to form hetero-oligomers (42). In addition, coexpression of the N- and C-terminal regions of the GFP protein alone yielded no fluorescence signal (Fig. 5*A*).

As expected, we observed a speckled GFP signal predominantly in the cytoplasm (in 96% of GFP-positive cells) when plasmids encoding GFP(1–157)-MxA and GFP(158–238)-MxA were co-transfected (Fig. 5*A*). We also observed that homodimerization of UAP56 or URH49 occurred primarily in the nucleus (in 92 and 92% of GFP-positive cells, respectively), also showing a speckled pattern (Fig. 5*A*). However, co-transfection of plasmids expressing GFP(1–157)-MxA

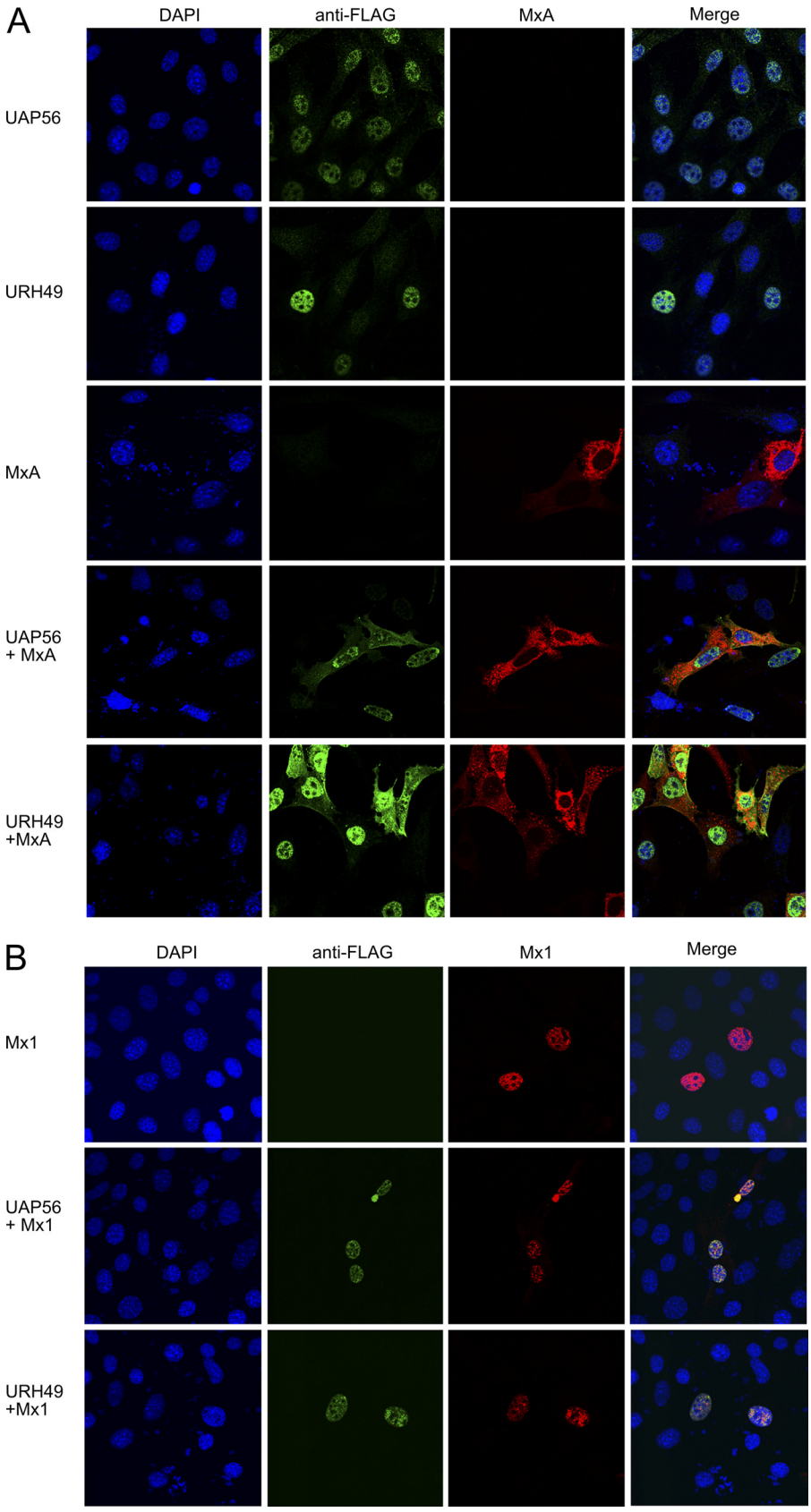

FIGURE 3. **Coexpression of MxA and UAP56 or URH49 leads to partial re-translocation of the helicases into the cytoplasm.** 3T3 cells were transfected with FLAG-tagged UAP56 or URH49 with or without MxA (*A*) or Mx1 (*B*). Cells were fixed with 4% formaldehyde and permeabilized with 0.5% Triton X-100. Cells were stained using anti-FLAG polyclonal antibody (1:2000) and anti-MxA antibody (1:20; clone 143). Images were taken with a Leica TCS SP5 confocal microscope.

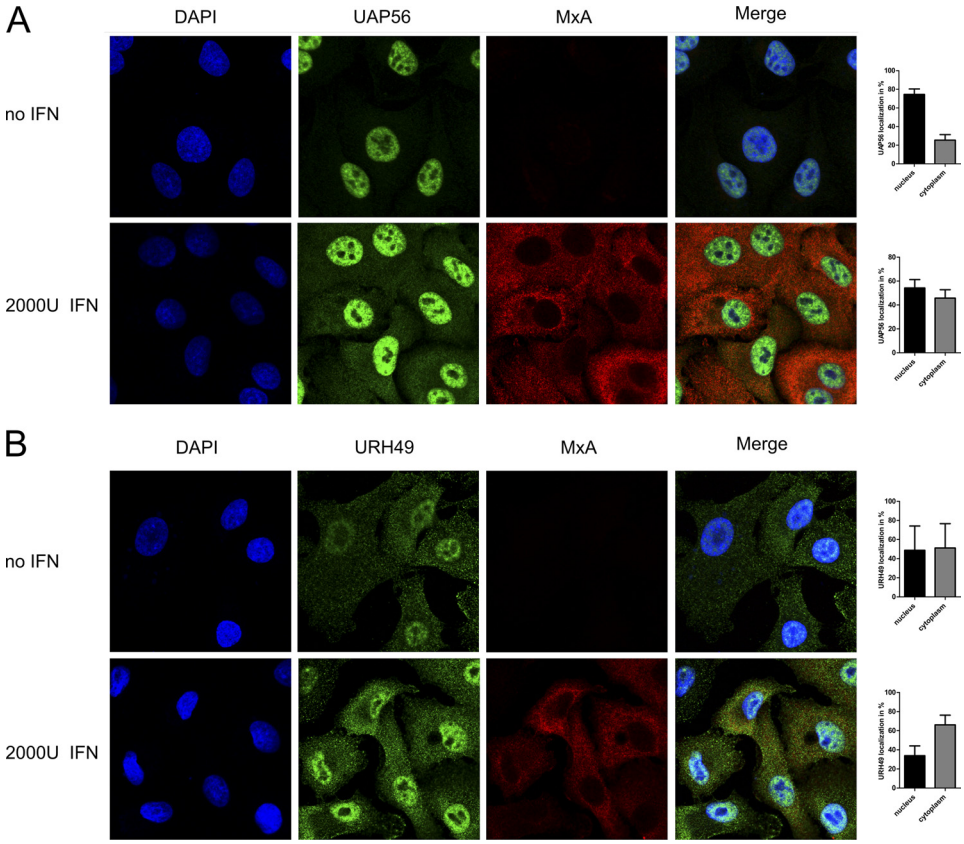

FIGURE 4. **Redistribution of UAP56 and URH49 in interferon-α-treated cells.** A549 cells were stimulated with 2000 units of interferon-α overnight and analyzed for a redistribution of UAP56 (*A*) or URH49 (*B*) as described in the legend of Fig. 3 using a Leica TCS SP5 microscope. Unstimulated cells were used as a control for both helicases. Quantification of the UAP56 (*A*) or URH49 (*B*) distribution was performed using ImageJ software.

and GFP(158–238)-UAP56 or GFP(158–238)-URH49 resulted in GFP signals located in the cytoplasm (in 95 and 96% of GFP-positive cells, respectively) (Fig. 5*A*). These results clearly indicate that the complex formation between MxA and the two RNA helicases occurs in the cytoplasm, supporting our data obtained from the immunofluorescence analysis, where we observed an increased translocation of UAP56 or URH49 into the cytoplasm in cells expressing MxA (see Figs. 3 and 4).

The mouse Mx1 protein accumulates in the nucleus and exhibits antiviral activity only against certain RNA viruses (all members of the *Orthomyxoviridae* family) with a replication step in this compartment (for review, see Ref. 4). Hence, coexpression of GFP(1–157)-Mx1 with GFP(158–238)-UAP56 or GFP(158–238)-URH49 yielded GFP signals almost exclusively in the nucleus (in 95 and 93% of GFP-positive cells, respectively) in the form of distinct dots (Fig. 5*B*).

DISCUSSION

Human MxA and mouse Mx1 proteins exert a pronounced antiviral activity against IAV (4), but, so far, no direct interaction between Mx proteins and IAV has been demonstrated. There is increasing evidence that the RNA helicases UAP56 and, in part, also URH49 are required for efficient IAV replication (18, 25, 27). UAP56 can bind to free NP as well as vRNPs of IAV (17, 18). UAP56 is involved in the nuclear export of several IAV mRNAs (26, 27). Moreover, UAP56 is also required during IAV replication to prevent the accumulation of dsRNA in the cytoplasm of infected cells (27). For IAV, no direct interaction between Mx proteins and viral proteins has so far been detected, and the molecular mechanism of Mx proteins against IAV remains elusive. Hence, on the basis of our results presented here, we propose that UAP56 might be the missing link between Mx proteins and the NP or vRNP of IAV. Here, we have shown that human MxA and murine Mx1 bind to UAP56 and URH49 *in vitro* as well as *in vivo*. Intriguingly, we observed a pronounced binding of MxA to UAP56 and URH49 in coimmunoprecipitation experiments despite the fact that MxA is located in the cytoplasm and UAP56 and URH49 are located predominantly in the nucleus (31, 33, 35). Our data clearly show that the interaction of MxA with UAP56/URH49 takes place in the perinuclear region of the cytoplasm (Fig. 5*A*). In this context, it is interesting to note that knockdown of UAP56 leads to the accumulation of dsRNA in the cytoplasm of IAV-infected cells (27). So far, all available evidence indicates that MxA protein exerts its antiviral function against IAV and other viruses in the cytoplasm (for review, see Ref. 1). There is no experimental evidence that MxA shuttles to the nucleus. Studies aimed at elucidating the step of influenza virus replication blocked by MxA revealed that it inhibits a poorly defined step following primary transcription of viral mRNA (43). Furthermore, forced expression of MxA in the nucleus by means of a foreign nuclear translocation signal resulted in an efficient inhibition of primary transcription of IAV, indicating that the nuclear form of MxA mimics the activity of mouse Mx1 (44). Hence, if MxA

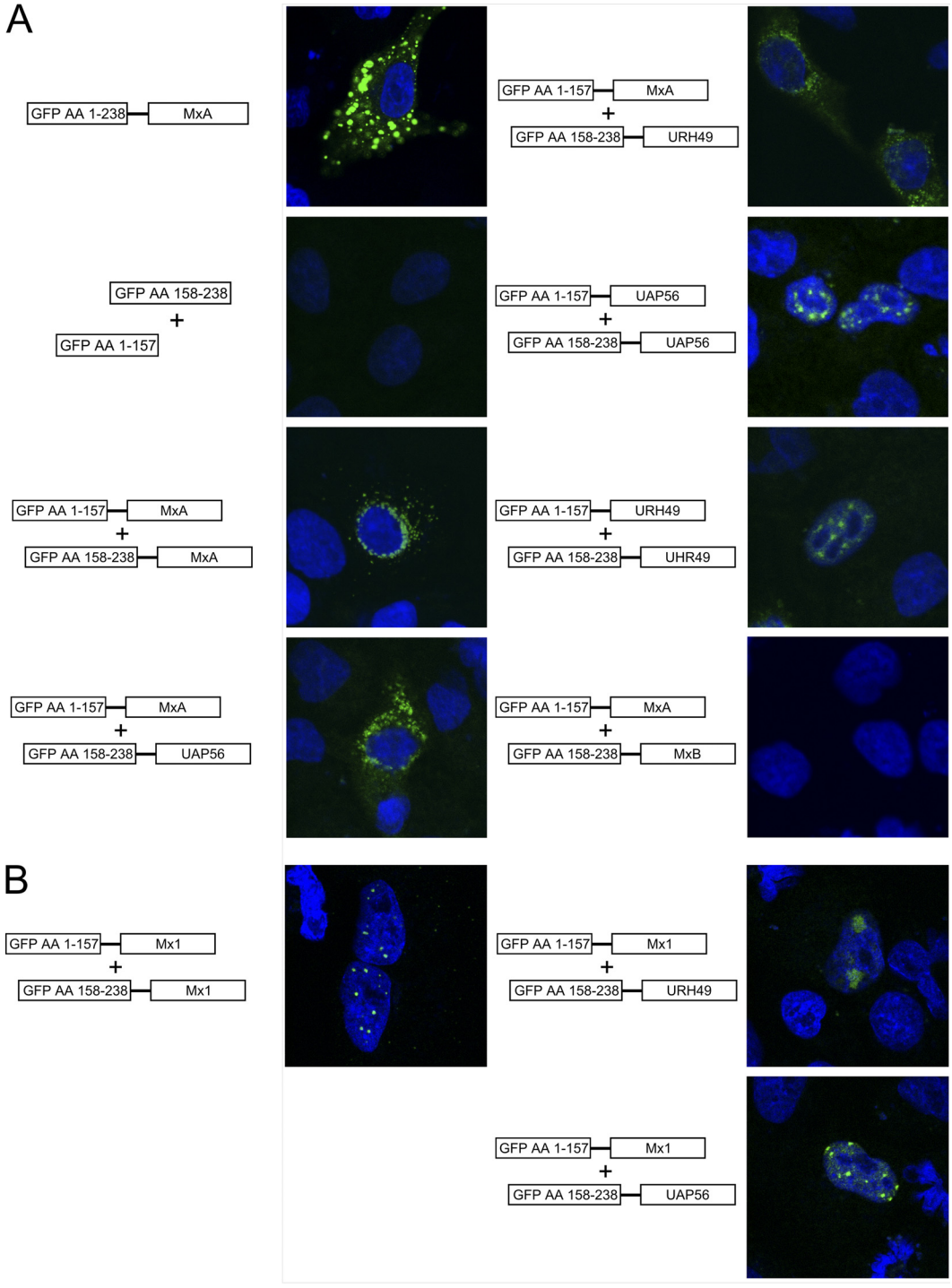

C

	total cells transfected	% in cytoplasm	% in nucleus
MxA x MxA	225	96	4
UAP56 x UAP56	239	8	92
URH49 x URH49	230	8	92
UAP56 x URH49	222	3	97
MxA x UAP56	233	95	5
MxA x URH49	209	96	4
MxA x MxB	241	0	0
GFP1-157 x GFP158-238	235	0	0
Mx1 x Mx1	236	6	94
Mx1 x UAP56	243	5	95
Mx1 x URH49	212	7	93

FIGURE 5. **Subcellular localization of the complexes formed between Mx proteins and UAP56 or URH49.** A549 cells were transfected with GFP(158–238)-UAP56 or GFP(158–238)-URH49 and MxA (*A*) or GFP(1–157)-Mx1 (*B*), resulting in GFP signal only upon protein-protein interaction. Coexpression of MxA and MxB was used as a negative control, as well as parental split GFP constructs without a protein fused to their C termini. Images were taken with a Leica TCS SP5 confocal microscope. *AA*, amino acids. *C*, quantification of the subcellular distribution of the protein-protein complexes formed given in percent of cells exhibiting GFP signals in the nucleus or cytoplasm. To identify transfected cells in the negative controls, cells were immunostained with antibodies directed against Mx proteins or GFP.

were to exert its anti-influenza activity in the nucleus, we would expect inhibition of primary transcription.

In addition, ectopically expressed UAP56 and URH49 showed a partial accumulation (partial retention) in the cytoplasm when coexpressed with MxA (Figs. 3 and 4). This was clearly not the case when both helicases were coexpressed with Mx1, which accumulated in the nucleus (Fig. 3). These data suggest that newly synthesized UAP56 and URH49 either are retained in the cytoplasm or are able to shuttle between the nucleus and cytoplasm. Indeed, Thomas *et al.* (45) have demonstrated that UAP56 and URH49 are nucleocytoplasmic shuttling proteins. In addition, two recent studies have demonstrated that UAP56 exhibits distinct activities in the cytoplasm, showing (i) that UAP56 is involved in proper translocation of mRNAs in the cytoplasm and (ii) that UAP56 exerts similar activity as eIF4A in protein translation in cardiomyocytes (34, 46).

The *in vitro* binding studies revealed that Mx1 bound to UAP56 or URH49 2–3-fold more efficiently than MxA (Fig. 2). In this context, it is interesting to note that Mx1 exhibits a more pronounced antiviral activity against IAV than MxA (28, 44, 47). However, it is also conceivable that, for nuclear Mx1, simply more UAP56 and URH49 are available because UAP56 and URH49 accumulate primarily in the cell nucleus.

Interestingly, *in vitro* binding of MxA or Mx1 protein to UAP56 or URH49 did not require GTP binding or GTP hydrolysis. The addition of GTP or its non-hydrolyzable analog GTPγS had no effect on the interaction efficiency (data not shown). However, the antiviral activity of Mx proteins requires at least GTP binding (28, 29). Hence, our findings indicate that binding of Mx proteins to UAP56 or URH49 appears not to represent the critical GTP-dependent step for antiviral function. The *in vitro* data further demonstrate that Mx1 binds more efficiently than MxA to UAP56 or URH49. It remains to be determined whether this difference in binding efficiency reflects the observed differences in antiviral activities against influenza viruses. Mx1 clearly shows a more pronounced restriction of influenza virus replication than MxA (2). Influenza virus strains were shown recently to differ in their sensitivities to Mx proteins (15). Taking advantage of the viral minireplicon system, Dittmann *et al.* (15) were able to determine that the sensitivity of influenza viruses to Mx proteins segregates with NP. Therefore, it will be interesting to test whether the different sensitivities of IAV strains to Mx proteins are reflected in different binding affinities for UAP56 and/or URH49.

Previous studies have demonstrated that the MxA protein associates with vRNP complexes of THOV, an influenza-related virus, and the NP protein of influenza virus (9, 48, 49). However, in none of these studies was a direct interaction of MxA and NP demonstrated. It is therefore conceivable that the observed association between the nucleocapsids of THOV and the NP protein of influenza virus is mediated by the cellular helicases UAP56 and/or URH49. In addition, MxA inhibits the replication of La Crosse virus by sequestering the N protein from the replication sites to perinuclear complexes (10). Hence, it will be interesting to test whether UAP56 and/or URH49 translocates together with MxA and the N protein to these perinuclear complexes.

We propose a new model for the antiviral activity of Mx proteins against influenza virus. In this model, Mx proteins block the replication of influenza virus (and possibly also other viruses) by physically interacting with the cellular helicases UAP56 and/or URH49 required for efficient viral replication. It remains to be determined whether Mx proteins act by simply sequestering the RNA helicases from NP or vRNPs or whether Mx proteins directly interfere with the function of UAP56 and/or URH49, *e.g.* by inhibiting their unwinding activity. It is conceivable that nuclear forms of Mx proteins such as mouse Mx1 may interfere with the maturation and nuclear export of viral mRNA in the nucleus, whereas cytoplasmic forms of Mx such as MxA may interfere with yet to be defined cytoplasmic activities of UAP56 and or/URH49. It also remains to be determined whether cytoplasmic forms of MxA proteins may interact with other cellular RNA helicases such as eIF4A, which is involved in translation of viral mRNAs.

Acknowledgments—We thank Alexandra Trkola and Friedemann Weber for helpful discussions, Urs Ziegler and Axel Mann for help with quantification of data, C. Basler and Peter Palese for kindly providing the cDNA for UAP56, and T. Stamminger for kindly providing the FLAG-URH49 expression construct.

REFERENCES

1. Haller, O., and Kochs, G. (2011) *J. Interferon Cytokine Res.* **31,** 79–87
2. Pavlovic, J., Zürcher, T., Haller, O., and Staeheli, P. (1990) *J. Virol.* **64,** 3370–3375
3. Frese, M., Kochs, G., Meier-Dieter, U., Siebler, J., and Haller, O. (1995) *J. Virol.* **69,** 3904–3909
4. Haller, O., Gao, S., von der Malsburg, A., Daumke, O., and Kochs, G. (2010) *J. Biol. Chem.* **285,** 28419–28424
5. Gao, S., von der Malsburg, A., Paeschke, S., Behlke, J., Haller, O., Kochs, G., and Daumke, O. (2010) *Nature* **465,** 502–506
6. Di Paolo, C., Hefti, H. P., Meli, M., Landis, H., and Pavlovic, J. (1999) *J. Biol. Chem.* **274,** 32071–32078
7. Janzen, C., Kochs, G., and Haller, O. (2000) *J. Virol.* **74,** 8202–8206
8. Schumacher, B., and Staeheli, P. (1998) *J. Biol. Chem.* **273,** 28365–28370
9. Kochs, G., and Haller, O. (1999) *Proc. Natl. Acad. Sci. U.S.A.* **96,** 2082–2086
10. Kochs, G., Janzen, C., Hohenberg, H., and Haller, O. (2002) *Proc. Natl. Acad. Sci. U.S.A.* **99,** 3153–3158
11. Engelhardt, O. G., Ullrich, E., Kochs, G., and Haller, O. (2001) *Exp. Cell Res.* **271,** 286–295
12. Horisberger, M. A. (1992) *J. Virol.* **66,** 4705–4709
13. Huang, T., Pavlovic, J., Staeheli, P., and Krystal, M. (1992) *J. Virol.* **66,** 4154–4160
14. Stranden, A. M., Staeheli, P., and Pavlovic, J. (1993) *Virology* **197,** 642–651
15. Dittmann, J., Stertz, S., Grimm, D., Steel, J., García-Sastre, A., Haller, O., and Kochs, G. (2008) *J. Virol.* **82,** 3624–3631
16. Zimmermann, P., Manz, B., Haller, O., Schwemmle, M., and Kochs, G. (2011) *J. Virol.* **16,** 8133–8140
17. Mayer, D., Molawi, K., Martínez-Sobrido, L., Ghanem, A., Thomas, S., Baginsky, S., Grossmann, J., García-Sastre, A., and Schwemmle, M. (2007) *J. Proteome Res.* **6,** 672–682
18. Momose, F., Basler, C. F., O'Neill, R. E., Iwamatsu, A., Palese, P., and Nagata, K. (2001) *J. Virol.* **75,** 1899–1908
19. Fleckner, J., Zhang, M., Valcárcel, J., and Green, M. R. (1997) *Genes Dev.* **11,** 1864–1872
20. Shen, H. (2009) *BMB Rep.* **42,** 185–188
21. Shen, H., Zheng, X., Shen, J., Zhang, L., Zhao, R., and Green, M. R. (2008)

Genes Dev. **22,** 1796–1803
22. Luo, M. L., Zhou, Z., Magni, K., Christoforides, C., Rappsilber, J., Mann, M., and Reed, R. (2001) *Nature* **413,** 644–647
23. Kapadia, F., Pryor, A., Chang, T. H., and Johnson, L. F. (2006) *Gene* **384,** 37–44
24. Pryor, A., Tung, L., Yang, Z., Kapadia, F., Chang, T. H., and Johnson, L. F. (2004) *Nucleic Acids Res.* **32,** 1857–1865
25. Kawaguchi, A., Momose, F., and Nagata, K. (2011) *J. Virol.* **85,** 6197–6204
26. Read, E. K., and Digard, P. (2010) *J. Gen. Virol.* **91,** 1290–1301
27. Wisskirchen, C., Ludersdorfer, T. H., Muller, D. A., Moritz, E., and Pavlovic, J. (2011) *J. Virol.* **17,** 8646–8655
28. Pitossi, F., Blank, A., Schröder, A., Schwarz, A., Hüssi, P., Schwemmle, M., Pavlovic, J., and Staeheli, P. (1993) *J. Virol.* **67,** 6726–6732
29. Schwemmle, M., Weining, K. C., Richter, M. F., Schumacher, B., and Staeheli, P. (1995) *Virology* **206,** 545–554
30. Accola, M. A., Huang, B., Al Masri, A., and McNiven, M. A. (2002) *J. Biol. Chem.* **277,** 21829–21835
31. Aebi, M., Fäh, J., Hurt, N., Samuel, C. E., Thomis, D., Bazzigher, L., Pavlovic, J., Haller, O., and Staeheli, P. (1989) *Mol. Cell. Biol.* **9,** 5062–5072
32. Stertz, S., Reichelt, M., Krijnse-Locker, J., Mackenzie, J., Simpson, J. C., Haller, O., and Kochs, G. (2006) *J. Interferon Cytokine Res.* **26,** 650–660
33. Kota, K. P., Wagner, S. R., Huerta, E., Underwood, J. M., and Nickerson, J. A. (2008) *J. Cell Sci.* **121,** 1526–1537
34. Meignin, C., and Davis, I. (2008) *Dev. Biol.* **315,** 89–98
35. Schmidt, U., Im, K. B., Benzing, C., Janjetovic, S., Rippe, K., Lichter, P., and Wachsmuth, M. (2009) *RNA* **15,** 862–876
36. Chelbi-Alix, M. K., Pelicano, L., Quignon, F., Koken, M. H., Venturini, L., Stadler, M., Pavlovic, J., Degos, L., and de Thé, H. (1995) *Leukemia* **9,** 2027–2033
37. Engelhardt, O. G., Sirma, H., Pandolfi, P. P., and Haller, O. (2004) *J. Gen. Virol.* **85,** 2315–2326
38. Ghosh, I., Hamilton, A. D., and Regan, L. (2000) *J. Am. Chem. Society* **122,** 5658–5659
39. Hu, C. D., Chinenov, Y., and Kerppola, T. K. (2002) *Mol. Cell* **9,** 789–798
40. Zhao, R., Shen, J., Green, M. R., MacMorris, M., and Blumenthal, T. (2004) *Structure* **12,** 1373–1381
41. Haller, O., and Kochs, G. (2002) *Traffic* **3,** 710–717
42. Melen, K., and Julkunen, I. (1997) *J. Biol. Chem.* **272,** 32353–32359
43. Pavlovic, J., Haller, O., and Staeheli, P. (1992) *J. Virol.* **66,** 2564–2569
44. Zurcher, T., Pavlovic, J., and Staeheli, P. (1992) *EMBO J.* **11,** 1657–1661
45. Thomas, M., Lischka, P., Muller, R., and Stamminger, T. (2011) *PLoS One* **6,** e22671
46. Sahni, A., Wang, N., and Alexis, J. D. (2010) *Biochem. Biophys. Res. Commun.* **393,** 106–110
47. Zurcher, T., Pavlovic, J., and Staeheli, P. (1992) *J. Virol.* **66,** 5059–5066
48. Kochs, G., and Haller, O. (1999) *J. Biol. Chem.* **274,** 4370–4376
49. Turan, K., Mibayashi, M., Sugiyama, K., Saito, S., Numajiri, A., and Nagata, K. (2004) *Nucleic Acids Res.* **32,** 643–652